Articles

Comparison of Sequence Preference of Tomaymycin- and Anthramycin–DNA Bonding by Exonuclease III and λ Exonuclease Digestion and UvrABC Nuclease Incision Analysis†

James R. Pierce,‡ Michael Nazimiec,§ and Moon-shong Tang*

M. D. Anderson Cancer Center, Science Park—Research Division, The University of Texas, Smithville, Texas 78957

Received December 22, 1992; Revised Manuscript Received April 28, 1993

ABSTRACT: The DNA bonding sites of two pyrrolo[1,4]benzodiazepine derivatives—tomaymycin (Tma) and anthramycin (Atm)—were identified by exonuclease III (exo III) digestion, λ exonuclease (λ exo) digestion, and UvrABC nuclease incision analysis. exo III digestion stalls 4-5 bases 3′ to a drug–DNA adduct. While this method can recognize most of the Atm- and Tma–DNA modification sites, it is complicated in that exo III digestion is also stalled by certain unmodified sequences and by drug bound to the opposite strand. λ exo digestion stalls 1-2 bases 5′ to a drug–DNA adduct. The λ exo method also recognizes most of the drug–DNA bonding sites and renders a cleaner background; however, it is also affected by opposite-strand drug bonding. Due to their intrinsic digestion polarities, these two exonucleases tend to be stalled by the drug–DNA adduct at one end of the DNA molecule. Purified UvrA, UvrB, and UvrC proteins acting together make dual incisions 6–8 bases 5′ and 4 bases 3′ to a Atm- or Tma–DNA adduct. This nuclease complex recognizes all the Tma- and Atm–DNA bonding sites identified by exonuclease digestion methods, and all the UvrABC incisions can be attributed to drug modifications in the incised DNA strand. The degree of UvrABC nuclease incision increases with increasing drug concentrations for DNA modification. Using the UvrABC incision method, we have identified the sequence preference of Tma- and Atm–DNA adduct formation in three DNA fragments, and we have found that these two drugs have different preferred sites for adduction. Both Tma- and Atm–DNA bonding is strongly influenced by the 5′ and 3′ neighboring bases; the orders of preferred 5′ and 3′ bases for Tma are A > G, T > C, and A, C > G, T, and for Atm the orders are A > G > T > C and A > G > T, C. The preferred triplets for Tma bonding are -AGA- > -GGC-, -TGC-, and AGC- and for Atm are -AGA-, -AGG- > -GGA-, -GGG-.

Tomaymycin (Tma) and anthramycin (Atm) (Figure 1), derivatives of pyrrolo[1,4]benzodiazepine (PB), are potent antitumor antibiotics produced by *Streptomyces tomaymyceticus* and *Streptomyces rufuineus*, respectively. These two drugs bond specifically through the C-11 of the drug molecule to the exocyclic 2-amino group of guanine in DNA (Petrusek et al., 1981; Barkley et al., 1986). Molecular modeling shows that the right-handed twist structures of these drugs fit snugly in the minor groove of B-form DNA and cause minimal distortion of DNA helix structure. Atm- and Tma–DNA bonding stabilizes the helix structure: DNA modified with Tma or Atm exhibits an increased melting temperature and is more resistant to S1 nuclease (Petrusek et al., 1981, Hurley & Thurston, 1984).

Although the mechanisms of covalent DNA bond formation by these two drugs are similar, it has been shown that more Atm than Tma can be bound to DNA, and DNA which has been saturated with Atm can still react with Tma. These results suggest that Atm and Tma may have different DNA sequence specificities (Hurley et al., 1977). The DNA sequence preference of bonding by these two drugs may play an important role in their different antitumor activities since these antibiotics do not bond to RNA and proteins (Hurley et al., 1977).

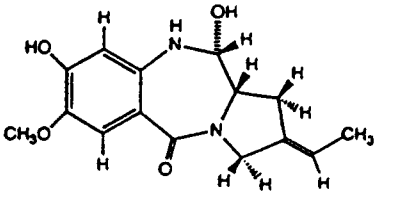

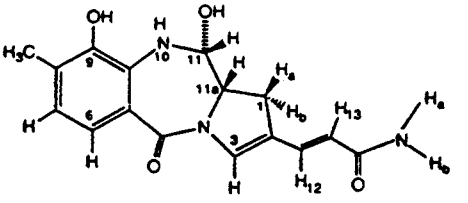

FIGURE 1: Chemical structures of tomaymycin and anthramycin.

The nucleotide site preferences for Tma- and Atm–DNA bonding have been partially determined by footprinting with methidium propyl-EDTA–iron(II) (MPE) and DNase I

† Supported by grants from the U.S. Public Health Service (ES03124, CA42897) and American Cancer Society (CH-485).

* To whom correspondence should be addressed.

‡ Present address: Department of Biology, Texas A&I University, Kingsville, TX 78363.

§ Present address: Department of Biochemistry and Biophysics, Texas A&M University, College Station, TX 77843-2128.

0006-2960/93/0432-7069$04.00/0

(Hertzberg et al., 1986). These techniques require using DNA modified with a high concentration of the antibiotics and, thus, are insensitive in detecting low-affinity modification sites in DNA. Furthermore, since drug bonding affects MPE and DNase I footprints on both bound and opposite, unbound DNA strands, determination of drug bonding sites in a sequence can be quite complex. Previously, we have shown that both λ exonuclease (λ exo) and exonuclease III (exo III) may be used to identify Atm bonding sites in DNA (Walter et al., 1988). These enzymes processively digest DNA from one end, either the 5′ end for λ exo or the 3′ end for exo III. When these enzymes encounter drug-modified bases, they tend to stall or be inhibited from further procession along the DNA strand. When modified DNA is treated with these enzymes and separated on a sequencing gel, bands are observed corresponding to bonding sites for the drug. These techniques can detect low levels of modification since the method relies on the appearance of a band or bands, rather than the disappearance of bands. In this report we have used these methods to identify the preferred Atm- and Tma–DNA bonding sequences.

Previously, we have reported that nucleotide incision proteins—UvrA, UvrB, and UvrC—isolated from *Escherichia coli* cells, working together, can incise at both the 5′ and 3′ sides of Atm–N2-guanine adducts (we term the collective function of these Uvr proteins the UvrABC nuclease). We identified more Atm bonding sites with this UvrABC nuclease incision method than with exo III and λ exo digestion methods (Walter et al., 1988). In this report, we show that UvrABC nuclease also incises Tma–N2-guanine adducts in the same fashion as Atm–N2-guanine. We have used UvrABC nuclease incision in addition to exonuclease digestion analysis to identify the preferred sequences for both Atm- and Tma-DNA bonding. The comparison shows that these two drugs have definite sequence preferences for bonding, and at several sites these two drugs differ substantially in the extent to which they bond. The advantages of using UvrABC nuclease incision to identify helix-stablizing drug-DNA bonding sites are discussed.

MATERIALS AND METHODS

Materials. Tomaymycin (NSC 177499) and anthramycin (NSC 106408, in methyl ester form) were obtained from the Natural Products Branch, Division of Cancer Treatment, National Cancer Institute. Restriction enzymes *Hae*II, *Hin*fI, *Nar*I, *Bam*HI, and *Eco*RI, T4 polynucleotide kinase, bacterial alkaline phosphatase, λ exonuclease, acrylamide, bisacrylamide, agarose, and NACS Prepacs convertible columns (NACS PACS) were obtained from Bethesda Research Laboratories. Restriction enzyme *Bst*NI and exonuclease III were obtained from New England Biolabs. Yeast tRNA was obtained from Sigma Chemical Co. All ^{32}P-labeled nucleotides were obtained from Amersham Co. or New England Nuclear.

DNA Fragment Isolation. Plasmid pBR322 was isolated and purified by cesium chloride density gradient centrifugation. The 174-bp *Eco*RI–*Hae*III 5′-end-^{32}P-labeled fragment was prepared from a 375-bp *Eco*RI–*Bam*HI fragment of pBR322 as described (Pierce et al., 1989). The 129-bp *Eco*RI–*Bst*NI 3′ end-^{32}P-labeled fragment was prepared from a 1857-bp *Bst*NI fragment of pBR322. The 174-bp 5′-end-labeled fragment and the 129-bp 3′-end-labeled fragment contain the same sequence of DNA from the unique *Eco*RI site to the *Bst*NI sites at base 129. Thus, by using these two labeled fragments, hydrolysis on either the 3′ side or the 5′ side of a damaged base could be estimated. The 247-bp *Hin*fI–*Bst*NI and the 238-bp *Nar*I–*Bst*NI 3′-end-^{32}P-labeled fragments of pBR322 were isolated from a 383-bp *Bst*NI fragment that had been agarose gel purified and 3′-end-labeled with [α-^{32}P]-TTP. The 952-bp *Bst*NI-*Bst*NI fragment of M13mp1 was 3′-end-labeled at position 952 with [α-^{32}P]TTP and purified on a 5% acrylamide gel.

Tomaymycin and Anthramycin Modification of DNA. Dry Tma was dissolved in methanol and the concentration determined by absorbance at 320 nm using the molar extinction coefficient of 3600 (Hurley et al., 1977). Dry Atm was dissolved in methanol and the concentration determined by absorbance at 333 nm using the molar extinction coefficient of 31 800 (Hurley et al., 1977). The drugs were then diluted in methanol and used to modify end-labeled DNA fragments. Appropriate dilutions of Tma or Atm were added to DNA in 0.1× SSC (15 mM NaCl and 1.5 mM sodium citrate, pH 7.0). The DNA–drug mixtures were incubated for 3 h at 25 °C before being precipitated with 3 volumes of ethanol in the presence of ammonium acetate (2.5 M) to remove the unreacted drug. The pellet was washed with 75% ethanol and dried in a Speed Vac (Savant Instruments).

Exonuclease Digestion of Tomaymycin- or Anthramycin-Modified DNA. Modified 5′-end-labeled DNAs were suspended in exo III buffer (50 mM Tris-HCl, pH 8.0, 5 mM $MgCl_2$, and 10 mM β-mercaptoethanol) and mofidified 3′-end-labeled DNAs were resuspended in λ exo buffer (67 mM glycine-KOH, pH 9.4, and 2.5 mM $MgCl_2$) as recommended by the vendors. To each DNA sample, 2 μg of a purified 4-kb *Eco*RI-*Bam*HI linear DNA fragment of pBR322 was added as carrier. Then, 50 units of exo III or 3 units of λ exo was added to each tube and incubation carried out for 30 min at 37 °C. The reactions were stopped by the addition of ammonium acetate (2.5 M) and 3 volumes of ethanol. After the samples were spun, in the microfuge, the DNA pellets were dried and dissolved in formamide denaturing dye mix (80% deionized formamide, 10 mM NaOH, 1 mM EDTA, 0.1% xylene cyanol, and 0.1% bromophenol blue) for electrophoresis.

UvrABC Nuclease Reactions. UvrA, UvrB, and UvrC proteins were purified from *E. coli* K12 strain CH296 carrying plasmids pUNC45 (*uvrA*), pUNC211 (*uvrB*), or pDR3274 (uvr*C*) (Tang et al., 1991). These plasmids and strain CH296 were kindly provided by Dr. A. Sancar. Incision of damaged DNA by Uvr proteins was done in 50 mM Tris-HCl, pH 7.5, 10 mM $MgCl_2$, 100 mM KCl, 1 mM ATP, and 1 mM DTT. An aliquot of ^{32}P-labeled DNA was reacted with 15 nM UvrA, 12 nM UvrB, and 15 nM UvrC in a volume of 25 μL for 90 min at 37 °C. The reaction was terminated by phenol extractions. The labeled DNA was then ethanol-precipitated, washed in 75% ethanol, dried, and dissolved in formamide denaturing dye mix.

Sequencing Reactions and Electrophoresis. Chemical sequencing was carried out as described by Maxam and Gilbert (1980) with the modifications described (Pierce et al., 1989). Sequencing gels, consisting of 8% acrylamide and 7 M urea in TBE buffer (50 mM Tris-HCl, 50 mM borate, and 10 mM EDTA, pH 8.3), were run on 0.4–0.8-mm wedge gels. The gels were dried in a Bio-Rad gel dryer and exposed to Kodak X-Omat RP films at −70 °C for various lengths of time. The intensity of bands was determined by scanning with a BioImage Visage 100 system, consisting of a high-resolution digitizing camera and whole band analysis software.

RESULTS

Identification of Tma- and Atm–DNA Bonding sites by exo III Digestion Analysis. exo III digests DNA processively

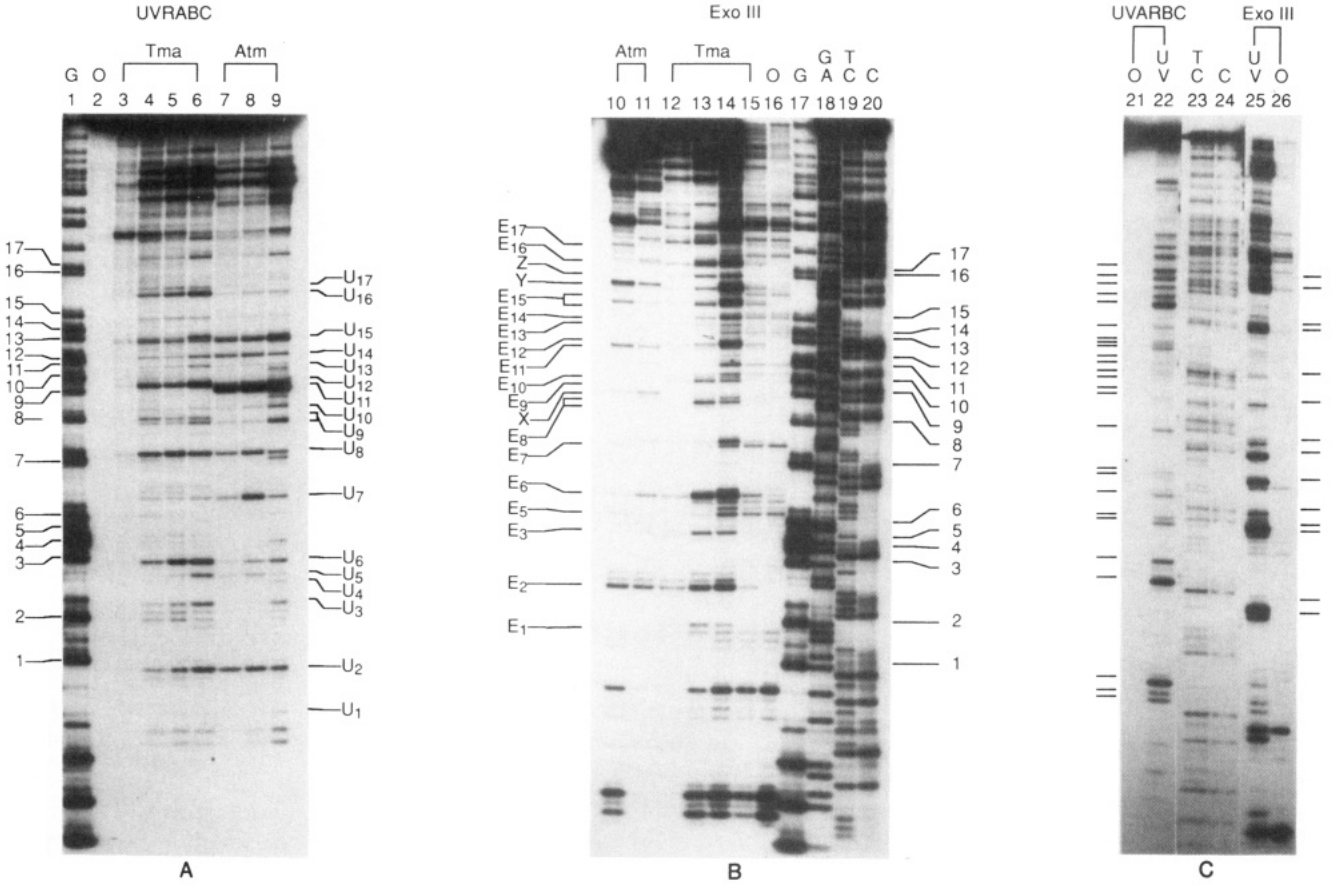

FIGURE 2: Electrophoresis of UvrABC nuclease and exo III treated Tma- (lanes 3–6 and 12–15), Atm- (lanes 7–11), or UV- (lanes 22 and 25) modified 5′-end-labeled (*Eco*RI–*Hae*III) 174-bp fragment. The DNA fragments with or without modifications were incubated with UvrABC nuclease (lanes 2–9, 21, and 22) or exo III (lanes 10–16, 25, and 26) as described in the text and then electrophoresed in an 8% sequencing gel. Lanes 1, 17–20, 23, and 24 are Maxam and Gilbert sequencing G, GA, TC, and C reactions. Lanes 2, 16, 21, and 26 are unmodified DNA, and lanes 22 and 25 are UV-treated DNA. Lanes 3 and 15, 4 and 14, 5 and 13, and 6 and 12 are DNA modified with 0.2, 2, 20, and 200 nmol of Tma. Lanes 7, 8 and 11, and 9 and 10 are DNA modified with 200, 20, and 2 nmol of Atm. The drug-induced exo III stop bands (E_1–E_{17}, X, Y, and Z) UvrABC nuclease incision bands (U_1–U_{17}) are labeled on the sides of the panels. The numbers correspond to the guanine residues which are numbered on the sides of the panels. In panel C the exo III stop bands (on the right) and the UvrABC incision bands (on the left) which have been identified with corresponding pyrimidine dimers are indicated by bars.

from the 3′-end of the molecule and this digestion stalls 3-4 bases 3′ to modified base(s). Methods based on this effect have been developed to identify sites of dichlorodiamineplatinum(II) and Atm modification and sites of photoproduct formation in DNA (Royer-Pokora et al., 1981; Walters et al., 1988). In brief, defined 5′-end-labeled DNA fragments modified with these agents were reacted with exo III, and the resultant fragments were separated by gel electrophoresis. Stops of exo III digestion on the DNA result in bands in the gel which correspond to fragments 3–4 bases larger than fragments which would be generated by cleavage at the site of modification. Analysis of the exo III stop sites, however, is complicated by the appearance of stop bands in unmodified DNA (Figure 2, lane 16). It is not clear why exo III produces stop bands in unmodified DNA. exo III digestion has been shown to proceed at different rates in different DNA sequences and to stall when encountering some sequences (Linxweiller & Horzi, 1982; Royer-Pokora et al., 1981). Nonetheless, exo III stop bands induced by base modifications can be identified by comparing modified DNA to the control DNA. Figure 2 (lanes 10–16) shows the results of electrophoretic separation of exo III digested 5′-end-labeled *Eco*RI–*Hae*III 174-bp DNA fragments modified with Tma (lanes 12–15) or Atm (lanes 10 and 11) or irradiated with UV (lane 25).

For Tma-modified DNA, 16 exo III stop sites (E_1–E_3, E_5–E_{10}, E_{12}–E_{16}, Z, and Y) were found in the readable region of the gel; these stop bands are labeled on the left side of panel B in Figure 2. These sites either were not present in the control lanes or showed a dose effect with increasing Tma modification levels. Fourteen bands (E_1–E_3, E_5–E_{10}, and E_{12}–E_{16}) correspond to positions 4 or 5 bases 3′ to a guanine residue, G1–G16, respectively, and we attributed these bands to stops of exo III digestion 4–5 bases 3′ to drug modifications at G1–G16. No Tma-induced stop sites were observed for G4, G11, or G17. The two bands Y and Z cannot be assigned to any guanine within 4 or 5 bases. However, they can be attributed to exo III digestion stops 4 bases 3′ to a cytosine (-GCT- [-AGC-] and -TCT- [-AGA-]). Since Tma bonds only to guanine, these three bands are probably due to stalling of exo III digestion caused by the modified guanines on the nonlabeled strand. Bands near the top of the gel in general are more intense than those near the bottom and exo III bands appear mostly near the top of the gel (Figure 2, lane 12) in DNA modified with higher concentrations of Tma. It is very likely that this is due to the polarity of exo III digestion rather than drug-DNA bonding affinity. Because of this end effect and the frequent stops attributable to opposite strand bonding, it is difficult to estimate sequence preferences for Tma modification using exo III alone.

exo III stop bands induced by Atm modifications in DNA are shown in lanes 10 and 11 in Figure 2 (E_2, E_3, E_5–E_7, E_{11}, E_{14}–E_{17}, X, and Y). These bands are located 4–5 bases 3′ to potential Atm bonding sites (guanine residues), as was observed for Tma-treated DNA. Although many of the same bands

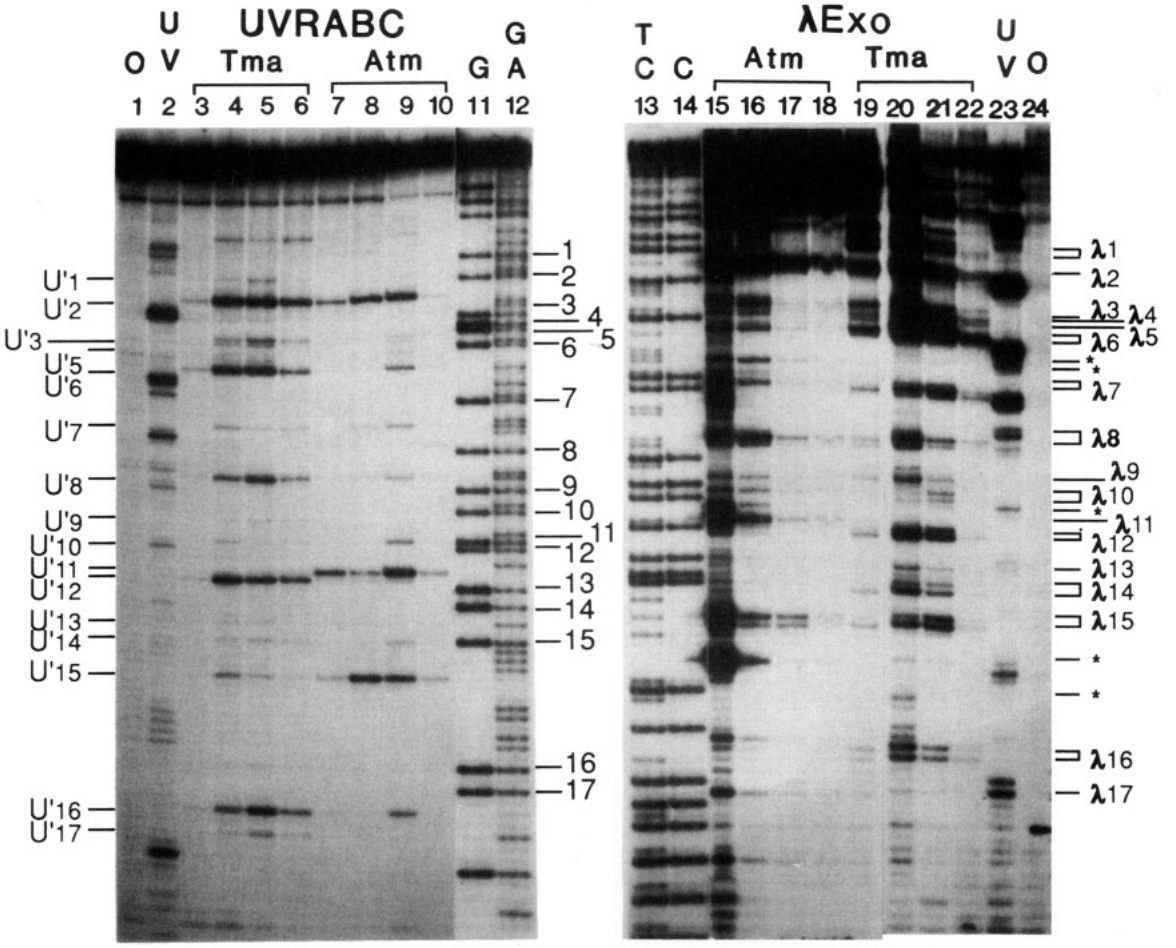

FIGURE 3: Electrophoresis of UvrABC nuclease (lanes 1–10) and λ exo (lanes 15–24) treated Tma- (lanes 3–6 and 19–22), Atm- (lanes 7–10 and 15–18), and UV- (lanes 2 and 23) modified 3′-end-labeled (*Eco*RI–*Bst*NI) 129-bp fragment. The DNA fragments with or without modifications were incubated with UvrABC nuclease (lanes 1–10) or λ exo (lanes 15–24) as described in the text and then electrophoresed in a 8% sequencing gel. Lanes 11–14 are Maxam and Gilbert sequencing reactions. Lanes 1 and 24 are unmodified DNA, and lanes 2 and 23 are UV irradiated DNA. Lanes 3 and 22, 4 and 21, 5 and 20, and 6 and 19 are DNA modified with 0.2, 2, 20, and 200 nmol of Tma, respectively. Lanes 7 and 18, 8 and 17, 9 and 16, and 10 and 15 are DNA modified with 200, 20, 2, and 0.2 nmol of Atm. The drug-induced λ exo stop bands (λ1–λ16) and UvrABC nuclease incision bands (U′1–U′17) are labeled on the sides of the panels. The numbers correspond to the guanine residues which are numbered on the sides of the panels.

noted in Tma-treated DNA were present in the Atm-treated DNA lanes, the intensity of some of the bands varies between the two drugs (E_3, E_5–E_7, and E_{16}). Except bands E_2, E_{15}, and Y, the bands seen in the Tma lanes are either very faint or absent in the Atm lanes. Conversely, there are some new bands in the Atm lanes that were not observed in the Tma lanes (X, E_{11}, and E_{17}). Band Y observed in Tma-modified DNA was also observed in Atm-modified DNA.

Results in Figure 2, lane 25, show that exo III stops in DNA irradiated with UV. There are 14 exo III stop bands which are 3–4 bases 3′ to all 15 of the potential pyrimidine dimer formation sites in the readable region of the gel (compare lane 25 to lane 23). It is noteworthy that there is no evidence of exo III stops due to pyrimidine dimers on the opposite strand. These results contrast with the results we have from both Tma- and Atm-modified DNA in which the exo III stops are attributable to drug-DNA adducts on the labeled strand as well on the opposite unlabeled strand.

Identification of Tma- and Atm–DNA Bonding Sites by λ Exo Digestion Analysis. λ exo, which digests DNA processively from the 5′-end of DNA, stalls 1–2 bases 5′ to modified bases. This enzyme has been used to identify Atm, mitomycin C, and (acetylamino)fluorene modification sites in DNA (Walter et al., 1988; Li & Kohn, 1991; Mattes, 1990). The λ exo experimental approaches are the same as those for the exo III digestion method except that 3′-end-labeled DNA is used instead of 5′-end-labeled DNA. Figure 3 shows the results of λ exo digestion of 3′-end-labeled DNA with Tma or Atm modification or with UV irradiation. In contrast to exo III, when unmodified control DNA is treated with λ exo (Figure 3, lane 24), there are almost no background bands. This could be due to the conditions of λ exo digestion, conducted at pH 9.4, which may eliminate certain DNA secondary structures. Alternatively, λ exo digestion may not be sensitive to DNA secondary structure. In Tma-modified DNA, λ exo stops 1 or 2 bases 5′ to the modification site (Figure 3, lanes 19–22). Stop bands accounting for Tma modification at 15 of the 17 examined guanines were identified. As in Figure 2, λ exo stop bands are labeled on the far right of the figure with λ_1–λ_{17}. There were no stop bands identified for G11 or G17. In many cases, λ exo stopped at both 1 and 2 bases 5′ to the modification site. This can be seen clearly at G's 1, 6, 7, 8, 10, 14, 15, and 16. This can complicate the identification of drug-modification sites, particularly in cases where there are two or more consecutive guanines. Similar to exo III digestion, the λ exo stop site intensities are skewed toward the 5′ end of the fragment, making estimations of site selectivity for Tma difficult. Also, just as was observed for exo III analysis of Tma adducts, λ exo appears to be stopped by bonding of Tma to the opposite strand. Two of the observed bands (marked with asterisks between λ15 and λ16) in the λ exo treated DNA lanes can be explained by stops at Tma adducts

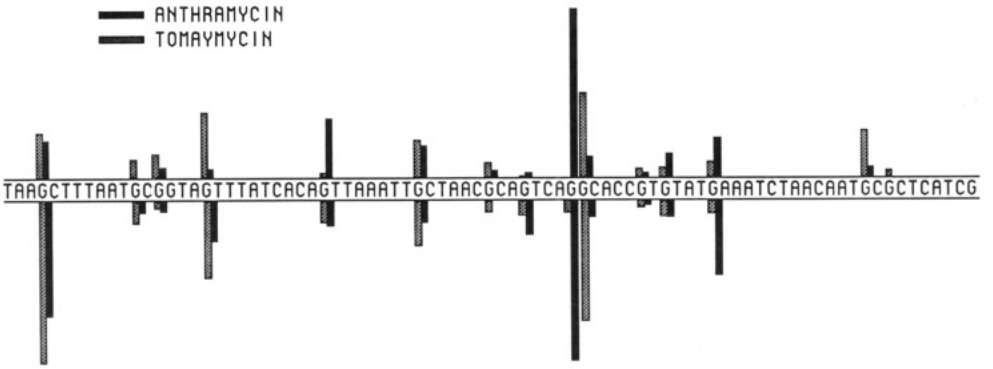

FIGURE 4: Relative intensity of UvrABC nuclease incisions on the 5′ and 3′ sides of drug–DNA adducts in the *Eco*RI–*Bst*NI 129-bp sequence. The intensities of UvrABC nuclease incision bands in lanes 5 and 8 in Figure 2 and lanes 5 and 9 in Figure 3 were scanned in a BioImage analyzer. The relative intensity (length of the bars) of each band was calculated as $B = I_i/\sum_{i=1}^{i} I_i$, where B is the relative intensity of each band and I_i is the reading of the individual band from the BioImage analyzer. Fourteen bands in the 3′-labeled DNA and 12 bands in the 5′-labeled DNA were calculated. The bars above and below the sequence represent the relative intensities of UvrABC nuclease incision at the 3′ and 5′ sides of the drug–DNA adduct, respectively.

bound to the opposite strand and are 2–3 bases 5′ to a cytosine. These two bands correlate with exo III stop sites (Z and Y) observed in the 5′-end-labeled DNA.

With Atm-modified DNA, λ exo recognized modifications at 12 of the 17 guanines studied (λ2–4, λ6–11, and λ15–17). λ exo stopped 1 or 2 bases 5′ to the bonding site. There were four bands that correlated with Atm bonding on the opposite strand (two bands marked with asterisks between λ6 and λ7, one between λ10 and λ11, and one between λ15 and λ16). As with the exo III analysis, with λ exo there were differences observed in the intensities of bonding between Atm- and Tma-treated DNA. Significantly, the same guanines (G11 and G12) showed the same differences in bonding shown by exo III. G11 bound no Tma and G12 bound no Atm.

Results in Figure 3, lane 23, show that λ exo digestion stops 1 or 2 bases 5′ to pyrimidine dimers and recognizes all of the 15 potential pyrimidine dimer sites in the readable region of this gel. As with exo III, there is no evidence of λ exo stops due to photoproducts on the opposite strand.

UvrABC Nuclease Incision on Tma- and Atm-Modified DNA. Although molecular modeling has demonstrated that both Tma and Atm fit snugly in the minor groove, it has been shown that the increase in DNA melting temperature and the extent of DNA curvature induced by Tma–DNA adducts is very different from that induced by Atm–DNA adducts (Hurley, 1977). These two drugs apparently have different effects on DNA helix structure. We have previously demonstrated that UvrABC nuclease makes dual incisions on both the 5′ and 3′ sides of the Atm-modified guanine in DNA; it is of interest to investigate whether or not UvrABC nuclease is able to incise Tma-modified DNA as it does Atm-modified DNA. To determine the incision sites of UvrABC nuclease on the 5′ side of drug–DNA adducts, 5′-end-labeled DNAs modified with Tma or Atm were reacted with UvrABC nuclease. Results in Figure 2 (lanes 2–9) show UvrABC nuclease incision bands in 5′-end-labeled DNA modified with Tma (lanes 3–6) or Atm (lanes 7–9). All bands corresponded to fragments generated that were 6–8 bases shorter than cleavage at a guanine position. These results suggest that UvrABC nuclease cuts 6–8 bases 5′ to Tma–N2-guanine as well as for Atm–N2-guanine. Fifteen UvrABC nuclease incision bands were observed corresponding to 17 potential Tma bonding guanine sites (no bands were observed for G4 and G11). The UvrABC incision bands are labeled on the right side of Figure 2A with capital letters U_1-U_{17}, with band U_1 corresponding to UvrABC incision about G1, U_2 corresponding to incision about G2, and so on. All the UvrABC incision bands can be attributed to Tma modifications on the labeled DNA strand. These results are the same as those we have found for Atm-modified DNA. There is significant variation in intensities of these bands, both within the Tma-modified DNA and between the Tma- and Atm-modified DNA.

To determine the UvrABC nuclease incision position on the 3′ side of drug–DNA adducts, 3′-end-labeled DNA modified with the drugs was reacted with UvrABC nuclease. Results in Figure 3 (lanes 3–10) show UvrABC nuclease incision bands in 3′-end-labeled DNA modified with Tma (lanes 3–6) or Atm (lanes 7–10). All bands correspond to fragments 4 bases smaller than fragments generated by cleavage at a guanine position. These results suggest that UvrABC nuclease cuts 4 bases 3′ to Tma–N2-guanine just as for Atm–N2-guanine. Incision bands are indicated on the left of Figure 3 and labeled with letters U'_1–U'_{17}, with band U_1' corresponding to UvrABC incision of G_1, U2′ corresponding to G_2, etc. Again, UvrABC recognizes Tma modification at all but two guanines (G4 and G11). All the UvrABC incision bands can be attributed to Tma modifications on the labeled DNA strand. These results are the same as those we have found for Atm-modified DNA, except that different guanines are modified. Significantly, there is a substantial variation in intensity among these bands.

Unlike exonuclease digestion on drug-modified DNA, UvrABC nuclease incision bands do not display a skewing of higher intensities toward the top or bottom of the gel. Furthermore, in DNA modified with high concentrations of the drugs, these bands are evenly reduced (see lanes 3–6 and 7–9 in Figure 2 and lanes 3–6 and 7–10 in Figure 3). These results suggest that DNA fragments modified with two or more drug molecules are not substrates for UvrABC nuclease. Figure 4 shows the densitometric scanning results from UvrABC incisions bands of Tma- and Atm-modified 5′- and 3′-end-labeled DNA. In general, the relative intensity of 5′ and 3′ incision bands for most of the drug-modified G's are similar; the G's which give strong 5′ UvrABC incision bands also give strong 3′ UvrABC incision bands. In addition, the sites that yield the strongest bands by UvrABC incision correspond to strong bands by exo III and λ exo. These results open the possibility that the intensity of the UvrABC nuclease incision bands represents the extent of drug–DNA adduct formation at the various positions and not the site preference for UvrABC incision (see below).

The degree of UvrABC cutting at many sites varies between the two drugs. For example, the bands indicating cutting at

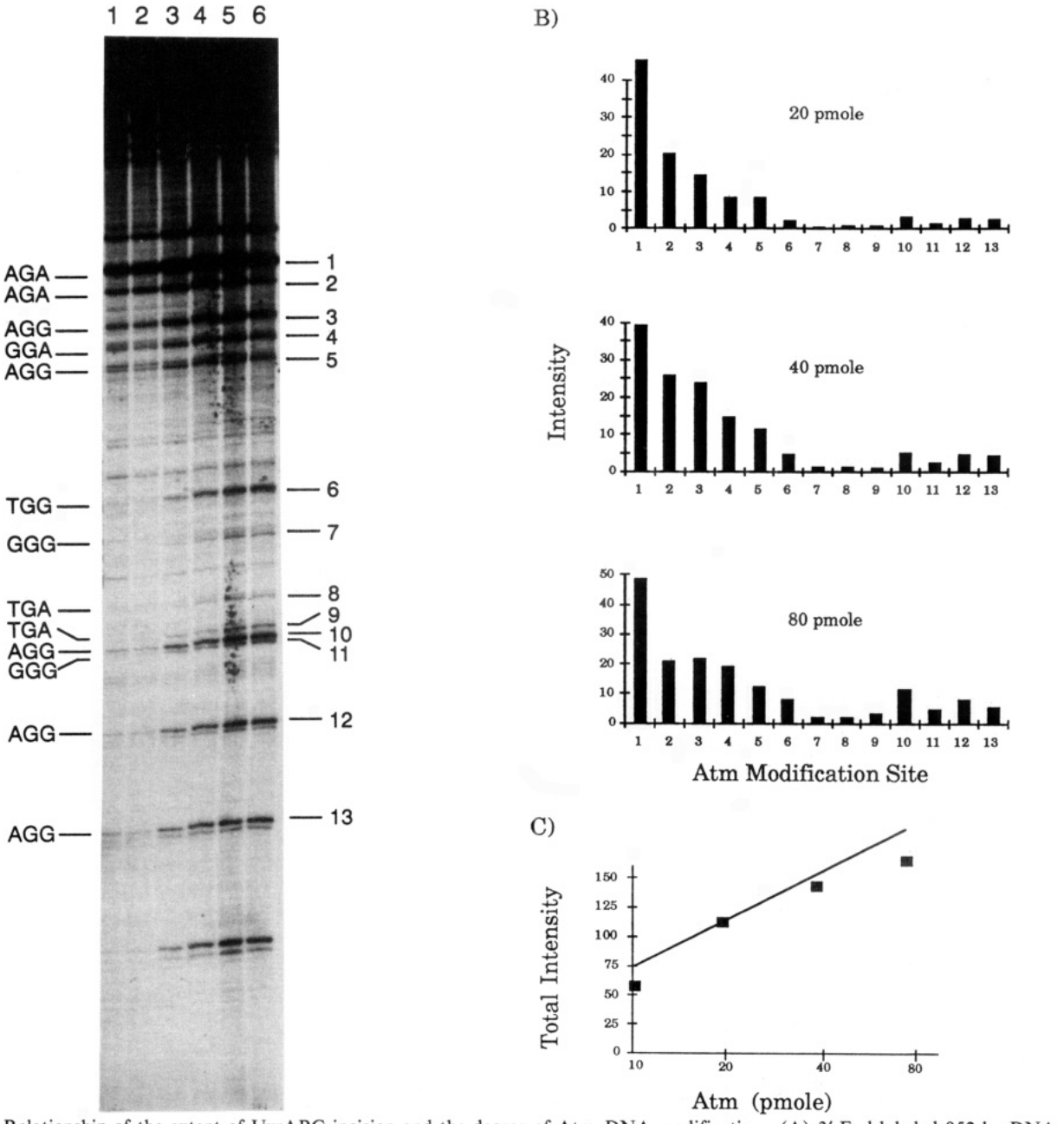

FIGURE 5: Relationship of the extent of UvrABC incision and the degree of Atm–DNA modification. (A) 3′-End-labeled 952-bp DNA fragments from M13mp1 were modified with 5, 10, 20, 40, 80, and 180 pmol of Atm (lanes 1–6) under standard conditions (see Materials and Methods). The modified DNA was reacted with excess UvrABC nuclease and the products were separated on a sequencing gel. (B) The relative intensity of individual bands obtained by densitometry from lanes with modification levels of 20, 40 and 80 pmol is shown. Site numbers correspond to the individual numbered bands in (A). (C) The total intensity of the 13 bands of (A) is plotted versus the Atm modification level in the standard reaction (0.1 ml final volume).

G6 and G16 are much more intense for Tma-modified DNA than for Atm-modified DNA, while the cutting bands for modification at G7 and G15 are much more intense for Atm-modified DNA than for Tma-modified DNA (Figure 2A). These results suggest that these two drugs have different sequence preferences for DNA bonding. It is worth noting that the concentration of Atm required to obtain optimal levels of drug bonding was approximately 1% of the concentration of Tma required to reach the same level of bonding (compare lanes 3–6 to lanes 7–9 in Figure 2).

Identification of the Bonding Spectra of Atm and Tma by UvrABC Nuclease Incisions. Since UvrABC nuclease incises all the Tma and Atm drug modification sites detected by λ exo and exo III digestions and there is no polarity effect in the enzyme incisions as displayed in the exo digestions (Figures 2 and 3), this enzyme system could have utility in identifying the sequence selectivity of DNA bonding of these two drugs.

The different band intensities presented in Figures 2 and 3 may be explained by two possibilities: one is that they reflect the efficiency of exonuclease stoppage or UvrABC incision at different sequences, assuming the drug modification at different sequences is random, and the other possibility is that they reflect the extent of drug modification at different sequences, assuming the UvrABC nuclease incises all DNA adducts at different sites with equal efficiency.

Neither of these extremes alone would be expected to account for the variation in UvrABC incision intensity from site to site, but rather each contributes, and in the absence of a direct measure of the number of adducts, it is difficult to assess their relative contributions. However, the following four experimental results provide evidence that the primary determinant of the UvrABC incision intensity is the degree

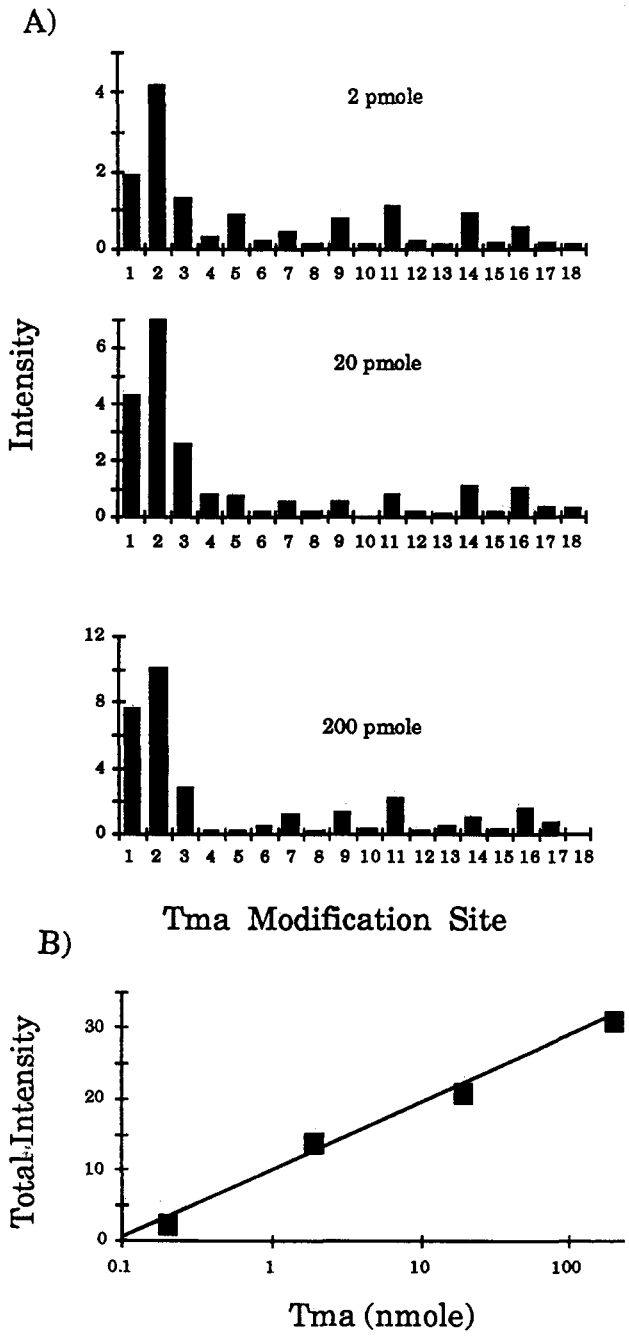

FIGURE 6: Relationship of the extent of UvrABC incision and the degree of Tma–DNA modification. (A) The relative intensity of individual bands obtained by densitometry from lanes with modification levels of 2, 20, and 200 nmol is shown. Site numbers correspond to the individual numbered bands in Figure 2. (B) The total intensity of the 18 bands of (A) is plotted versus the Tma modification level in the standard reaction (0.1 ml final volume).

of adduct formation at the site. First, Tma and Atm do not bind to DNA randomly, since the MPE footprint technique has shown that Atm binds to -PuGPu- sequences preferentially and Tma binds to triplets (excluding PuGPu) with a frequency much lower than 50% (Hertzberg et al., 1986). Our results based on the intensity of UvrABC cutting are consistent with this limited site preference. Second, we find the intensity of UvrABC incision is dose-dependent for Atm and Tma and that the relative intensities at different sites remain proportional with increasing modification levels (Figures 5 and 6). This is most easily interpreted as increasing UvrABC incision with increasing modification at the site. The sites which show the high modifications at low drug concentrations show smaller increases in incision level, as if they were reaching saturation with the drug. Third, the relative intensities of drug-induced UvrABC bands are in good agreement with the relative intensities of drug-induced exo III and λ exo bands (Figure 7). Since a different enzyme–DNA interaction is expected for these different systems, the agreement in intensities probably correlates with the modification level at the drug site. Last, at the sequence -CTGGTA- in the 247-bp DNA, the first G is recognized by both the exonucleases and UvrABC as modified by Atm while the second is not; conversely, the second G is recognized as modified by Tma while the first is not. (A similar occurrence is found in the 174-bp sequence; Figure 2.) This difference is best accounted for by the modification of respective G's by the drugs rather than a consequence of identical sequence specificity of UvrABC and the exonucleases.

Accepting the validity of UvrABC incision method in determining the DNA bonding affinity at different sequences, we then investigated drug–DNA bondings in two more DNA fragments (*Hin*fI–*Bst*NI, 247 bp, and *Nar*I–*Bst*NI, 238 bp) for the purpose of obtaining statistically relevant numbers of drug–DNA bonding sites. These fragments were 3′-labeled, modified with drugs, and subsequently reacted with UvrABC nucleases. Again, the drug-induced UvrABC incision bands do not show higher intensities near the sequence termini, as is found with exonuclease analysis, and there are substantial differences in band patterns between Atm- and Tma-modified DNAs (data not shown). The three DNA sequences accessible from autoradiographs spanned over 500 bases and included 103 guanines and afforded a random distribution of bases and triplet sequences. Using the MPE footprinting technique, Hertzberg et al. (1986) have previously assessed the sequence preference of drug–DNA bonding activities by the frequency of drug-induced footprints at different sequences; however, the extent of drug–DNA bonding at different sequences within a DNA fragment has not been addressed. Since in the UvrABC analysis most guanines within the readable portions of the gels were found to be modified, the frequency of modification at a trinucleotide is essentially equal to the frequency of occurrence of that trinucleotide in the set except for a few infrequently modified guanines. The frequency and intensity analyses agree well on which nucleotide triplets contain poorly modified guanines. The existence of bands with a wide range of intensities after UvrABC incision allows us to make a more detailed analysis. The distinctly different intensities of drug-induced UvrABC nuclease incision bands shown in Figures 2, 3, and 5 suggest that this method may be able to quantify the sequence specificity of drug–DNA bonding. Therefore, we have compared the bonding activities for both Atm and Tma by the relative intensity of UvrABC nuclease incision at these different sequences. The results are analyzed on the basis of both the dinucleotide sequences $-N_uG^*-$ and $-G^*N_u-$ and the trinucleotide sequences $-N_uG^*N_u-$, where G* is the drug bonding guanine residue. Table I lists the results for the dinucleotide sequences analysis; it reveals that bases flanking the guanine modification site play an important role in the drug bonding process. The relative intensity analysis demonstrates that for Tma-DNA bonding, adenine is clearly the preferred nucleotide 5′ to the drug site and the reactivity order for the 5′ base is A > G, T > C. Correspondingly, an adenine or cytosine 3′ to the drug bonding locus led to increased Tma-DNA bonding. The order of the reactivity for the 3′ base is A or C > T or G. For Atm–DNA covalent bond formation, adenine is the preferred base on both the 5′ and 3′ sides of the reactive guanine. The reactivity orders for the 5′ base and the 3′ base are A > G > T > C and

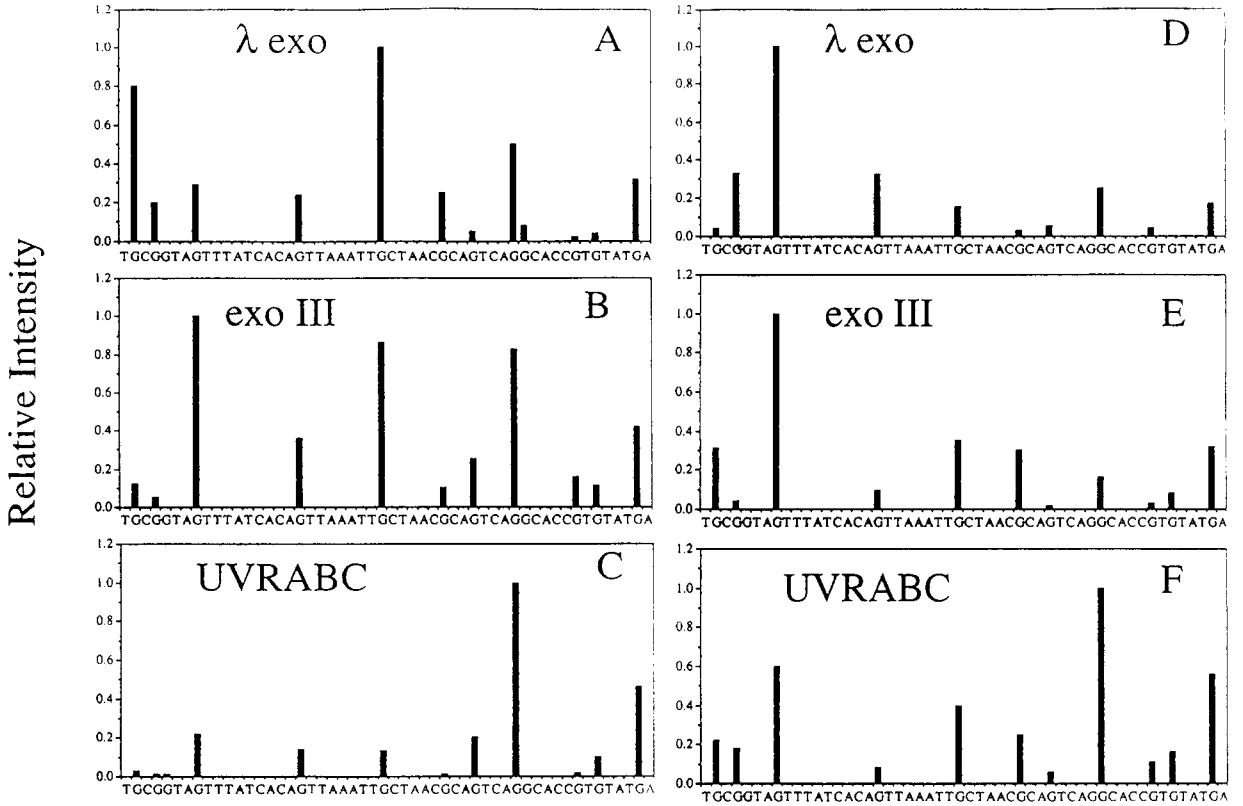

FIGURE 7: Relative intensities of Atm- (A–C) and Tma- (D–F) induced λ exo, exo III, and UvrABC nuclease incision bands in the *Eco*RI–*Bst*N1 129-bp pBR322 fragments. The band intensities of E_3–E_{15} of Figure 2, lanes 10 and 14, λ3–λ15 of Figure 3, lanes 15 and 20, and U3–U15 of Figure 3, lanes 5 and 9, were normalized to the intensity of the highest band. These bands were chosen for comparison because they show the least polarity effect.

Table I: Dinucleotide Analysis[a]

sequence[c]	no.	relative intensity ± SE[b] Tma	Atm
-NuG*-			
AG	19 (24)	5.2 ± 1.7 (5.0 ± 1.5)	6.9 ± 1.8 (6.8 ± 1.5)
GG	23 (25)	2.9 ± 1.3 (2.9 ± 1.2)	1.9 ± 0.7 (1.7 ± 0.6)
TG	16 (21)	1.4 ± 0.6 (2.5 ± 0.8)	0.7 ± 0.3 (1.3 ± 0.4)
CG	27 (33)	0.8 ± 0.4 (0.8 ± 0.3)	0.2 ± 0.1 (0.2 ± 0.1)
-G*Nu-			
GA	22 (26)	3.4 ± 1.6 (3.7 ± 1.5)	4.1 ± 1.2 (4.1 ± 1.2)
GG	22 (24)	1.3 ± 0.7 (1.2 ± 0.6)	2.9 ± 1.2 (3.3 ± 1.2)
GT	9 (16)	0.7 ± 0.3 (1.3 ± 0.6)	0.2 ± 0.1 (0.9 ± 0.3)
GC	31 (38)	3.1 ± 1 (3.5 ± 0.8)	0.6 ± 0.3 (1 ± 0.4)

[a] The analyses were based on results from *Hin*fI–*Bst*NI 247-bp and *Nar*I–*Bst*NI 238-bp DNA fragments with and without an additional *Eco*RI–*Bst*NI 129-bp fragment. Only the lanes which show the highest UvrABC incision were quantified. Since the length difference between the *Hin*fI–*Bst*NI 247-bp and *Nar*I–*Bst*NI 238-bp fragments is small and both were labeled at the same *Bst*NI site, these two fragments were assumed to have the same ^{32}P specific activity. Furthermore, the conditions for drug modification and UvrABC reaction are identified for these two DNA fragments, and the same amounts of DNA were applied in each lane for electrophoresis. Thus, the intensities of drug-induced UvrABC incision bands between these two DNA fragments were compared directly. To include the results from the *Eco*RI–*Bst*NI 129-bp fragment (labeled at the *Bst*NI site) into the statistical analysis, the intensities of drug-induced UvrABC incision bands were normalized to a length of 247 bp and average data from all three sequences are shown in parentheses. [b] Relative intensity (RI) of drug-induced UvrABC nuclease incision bands. [c] G* represents the drug-modified guanine residue.

A > G > T, C, respectively.

Table II presents the results of trinucleotide sequences analysis and the relative intensities for Tma–DNA bonding were grouped into three categories: highest bonding (>10), strong bonding (3–9), and weak bonding (<3). These analyses reveal two aspects which either differ from or were not observed

Table II: Trinucleotide Analysis[a]

-NuG*Nu-[c]	no.	relative intensity ± SE[b] Tma	Atm
AGA	5 (5)	11.1 ± 5.4 (11.1 ± 5.4)	12.2 ± 4.0 (12.2 ± 4.0)
GGC	11 (12)	4.4 ± 2.5 (4.5 ± 2.3)	0.1 ± 0.1 (0.1 ± 0.1)[d]
TGC	5 (8)	3.7 ± 1.3 (4.4 ± 0.9)	0.5 ± 0.3 (1.1 ± 0.5)
AGC	7 (8)	3.2 ± 1.8 (4.7 ± 1.8)	1.9 ± 1.0 (3.0 ± 1.5)
GGA	5 (5)	3.1 ± 2.9 (3.1 ± 2.9)	5.8 ± 2.0 (5.8 ± 2.0)
AGG	5 (6)	2.8 ± 2 (2.4 ± 1.7)	10.6 ± 3.6 (11.2 ± 3.0)
CGG	9 (10)	1.4 ± 1.2 (1.3 ± 1)	0.04 ± 0.04 (0.1 ± 0.05)
TGT	2 (3)	1 ± 1 (1 ± 0.5)	0.3 ± 0.3 (0.7 ± 0.5)
TGG	2 (3)	1 ± 1 (1.2 ± 0.6)	0 (0)
AGT	2 (5)	0.8 ± 0.8 (2.6 ± 1.9)	0.6 ± 0.6 (2 ± 0.6)
GGT	3 (4)	0.7 ± 0.7 (0.6 ± 0.6)	0.17 ± 0.7 (1.3 ± 0.8)
CGA	7 (8)	0.5 ± 0.4 (0.5 ± 0.3)	0.2 ± 0.1 (0.2 ± 0.1)
CGC	9 (11)	0.4 ± 0.2 (0.6 ± 0.2)	0.3 ± 0.3 (0.3 ± 0.3)
CGT	2 (4)	0.4 ± 0.4 (0.6 ± 0.2)	0 (0)
GGG	4 (4)	0.4 ± 0.4 (0.4 ± 0.4)	2.6 ± 1.1 (2.6 ± 1.1)
TGA	5 (6)	0.3 ± 0.1 (2.4 ± 2.1)	1.7 ± 0.7 (2.5 ± 1)

[a] The analysis is the same as in Table I. [b] Relative intensity of drug-induced UvrABC nuclease incision bands. [c] G* represents the drug-modified guanine residue. [d] Ten sites were analyzed for Atm.

by the MPE footprinting technique (Hertzberg et al., 1986): One is that Tma shows a clear sequence selectivity in DNA bonding; the preferred trinucleotides are -AGA-, -GGC-, -TGC-, and -AGC-. The second aspect is that although the four -P_uGP_u-trinucleotides are the preferred Atm bonding sites, Atm bonds more strongly in the sequences -AGA-, -AGG-, and -GGA- than in the -GGG- sequence.

DISCUSSION

Using exo III and λ exo digestion analysis, we were able to identify Tma and Atm modification sites in DNA fragments; however, not all modification sites can be reliably identified

by these methods and the analysis can be complicated by stop sites caused by drug bound to the opposite strand and (particularly for exo III digestion) by certain DNA sequences. In contrast, the UvrABC nuclease was able to detect all of the bonding sites detected by the exonucleases and more; moreover, all the Atm- and Tma-induced UvrABC nuclease incision bands can be attributed to drug bound on the same strand of the DNA. UvrABC nuclease apparently recognizes the modified strand and is not "confused" by drug bound on the opposite strand of the DNA. Furthermore, UvrABC nuclease incision does not show the polarity effect which is seen with the exonuclease. Therefore, these results indicate that the UvrABC nuclease incision method is superior to the exonuclease digestion methods in identifying and quantifying Atm– and Tma–DNA bonding.

The reason why only certain drug modification sites on the off-strand stop exonuclease digestion on the on-strand is unclear. Nonetheless, these results indicate that drug bonding at different sequences can affect the DNA structure differently. Presumably, interference by adducts on the opposite strand is a problem general to adducts that stabilize DNA helix structure or that interact with both strands; CC-1065–N3-adenine DNA adducts which stabilize DNA helix structure also cause the same interference (data not shown). On the other hand, pyrimidine dimers (Figures 2 and 3) and *N*-(deoxyguanosin-C8-yl)-2-aminofluorene (dG-C8-AF) and *N*-(deoxyguanosin-C8-yl)-2-(acetylamino)fluorene (dG-C8-AAF) adducts (data not shown) which destabilize DNA helix structure only stall exonuclease digestions on the same strand but not on the opposite strand.

The sequence specificity of Atm– and Tma–DNA bonding was evident not only in UvrABC nuclease incision lanes but also in exonuclease digestion lanes when DNAs modified with optimal levels of drugs were used as substrates (lanes 10 and 13 in Figure 2 and lanes 16 and 21 in Figure 3). Presumably, if the number of drug modifications per DNA fragment is 1 or less than 1, then the sequence specificity of drug–DNA bonding can be identified by exonuclease digestion analysis. Generally, guanines that result in more intense bands in the exo lanes also result in more intense bands in the UvrABC lanes (Figures 2, 3, and 7). The agreement of the three methods strongly suggests that the observed sequence selectivity lies in the bonding by the drugs to specific sequences of DNA rather than in any variation in the efficiency of exonucleases or UvrABC nuclease in detecting bonding at different sequences. The sequence independence of UvrABC nuclease incision has also been observed with other bulky chemical induced DNA damage (Sancar et al., 1985; Pierce et al., 1989; Tang et al., 1992).

Although Atm and Tma share one preferred bonding site, -AGA-, they show great discrepancy in bonding at several sites such as -GGC-, -GGG-, and -TGC- in the three defined DNA sequences we have examined. There are many sites that apparently fail to bond to Atm to which Tma bonds and vice versa. These results are consistent with the report that in bulk DNA, Atm bonding sites do not appear to completely overlap with Tma bonding sites (Barkley et al., 1986); i.e., DNA saturated with Atm is still capable of bonding Tma. The nearest-neighbor analysis of Tma and Atm bonding sites indicates that the bases at both 5′ and 3′ sides of a guanine are critical for the Atm and Tma bonding process. The results were unexpected since Hertzberg et al. (1986) were unable to detect preferred sequences for Tma–DNA adduction. This may be due to the limitations of the footprinting method used by these workers, which has difficulty quantifying the degree of drug bonding at individual sites; in contrast, the intensity of the distinct UvrABC nuclease incision band induced by each drug bonding site is easily quantified.

Although an adenine immediately adjacent on the 5′ and 3′ side of guanine is the preferred site bonding by both drugs, the other bases also have significant effects on bonding by these two drugs. For example, guanine on the 3′ side is the least favorable sequence for Tma bonding, but it is a favorable sequence for Atm bonding. These results suggest that there are some common features which govern Atm– and Tma–DNA bonding but there are also factors which affect Atm– and Tma–DNA bonding differently.

We observed that, compared to Atm, a much higher Tma concentration is needed for DNA modification to reach a similar extent of incision by UvrABC (Figures 2, 3, 5, and 6). Using spectroscopic measurements, Hurley et al. (1977) reported that Atm has a higher affinity for DNA bonding than Tma. Thus UvrABC nuclease probably does not recognize Atm–DNA adducts better than Tma–DNA adducts, but it is more likely that Atm has a higher DNA bonding affinity than Tma has under our conditions of modification.

Finally, our results show that UvrABC nuclease makes identical dual incisions at 6–8 bases (with most cases at 7 bases) 5′ and 4 bases 3′ to Atm– and Tma–DNA adducts, even though these two kinds of drug–DNA adducts have different effects on DNA helix structures. Previously we have reported that the UvrABC nuclease makes dual incisions 5–6 bases 5′ and 4–5 bases 3′ to Atm–DNA adducts (Walter et al., 1988). This discrepancy is due to a previous misalignment of the gels. UvrABC nuclease also makes the same dual incisions on a number of DNA damages such as cyclobutane pyrimidine dimers, dG-C8-AAF, benzo[*a*]pyrene diol epoxide–N2-guanine, dG-C8-AF, thymine glycol, and *O*6-methylguanine (Sancar & Rupp, 1983; Yeung et al., 1983; Sancar et al., 1985; Lin & Sancar, 1989; Voigt et al., 1989; Pierce et al., 1989; Kow et al., 1990; Tang et al., 1992). While the former three DNA adducts disrupt base pairings, the latter three adducts do not. Pyrimidine dimers have been shown to cause DNA bending and unwinding; dG-C8-AAF and benzo[*a*]pyrene diol epoxide–DNA adducts cause DNA unwinding. In contrast, Atm and Tma apparently do not change the helix structures significantly. That UvrABC nuclease is able to make such uniform incisions on a variety of DNA damages suggests that the UvrABC nuclease may process DNA damage to a common structure before making incisions.

In summary, we have found that UvrABC nuclease makes the same dual incisions on Atm– and Tma–DNA adducts. Using the UvrABC nuclease incision method in combination with exonuclease digestion analysis, we are able to determine the sequence specificity of bonding of these drugs and show that there are significant differences in the sequence preference in DNA bonding between these two drugs.

REFERENCES

Barkley, M. D., Cheatham, S., Thurston, D. E., & Hurley, L. H. (1986) *Biochemistry 25*, 3021–3031.

Hertzberg, R. P., Hecht, S. M., Reynolds, V. L., Molineux, I. J., & Hurley, L. H. (1986) *Biochemistry 25*, 1249–1258.

Hurley, L. H. (1977) *J. Antibiot. 30*, 349–370.

Hurley, L. H., & Thurston, D. E. (1984) *Pharm. Res. 1*, 53–59.

Hurley, L. H., Gairola, C., & Zmijewski, M. (1977) *Biochim. Biophys. Acta 475*, 521–535.

Kow, Y. Y., Wallace, S. S., & Van Houten, B. (1990) *Mutat. Res. 235*:147–156.

Li, V.-S., & Kohn, H. (1991) *J. Am. Chem. Soc. 113*, 275–283.

Lin, J.-J., & Sancar, A. (1989) *Biochemistry 28*, 7979–7984.

Linxweiler, W., & Horzi, W. (1982) *Nucleic Acids Res. 10*, 4845–4895.
Mattes, W. B. (1990), *Nucleic Acids Res. 18*, 3723–3730.
Maxam, A. M., & Gilbert, W. (1980) *Methods Enzymol. 65*, 499–560.
Petrusek, R. L., Anderson, G. L., Garner, T. F., Fannin, W. L., Kaplan, D. J., Zimmer, S. G., & Hurley, L. H. (1981) *Biochemistry 20*, 1111–1119.
Pierce, J. R., Case, R., & Tang, M.-s. (1989) *Biochemistry 28*, 5821–5826.
Royer-Pokora, B., Gordon, L. K., & Haseltine, W. A. (1981) *Nucleic Acids 9*, 4595–4609.
Sancar, A., & Rupp, W. D. (1983) *Cell 33*, 249–260.
Sancar, A., Franklin, K. A., Sancar, G., & Tang, M.-s. (1985) *J. Mol. Biol. 184*, 725–734.
Tang, M.-s., Nazimiec, M., Doisy, R. P., Pierce, J. R., Hurley, L. H., & Alderete, B. E. (1991) *J. Mol. Biol. 220*, 855–866.
Tang, M.-s., Pierce, J., Doisy, R., Nazimiec, M., & MacLeod, M. (1992) *Biochemistry 31*, 8429–8436.
Voigt, J. M., Van Houten, B., Sancar, A., & Topal, M. D. (1989) *J. Biol. Chem. 264*, 5172–5176.
Walter, R. B., Pierce, J. R., Case, R., & Tang, M.-s. (1988) *J. Mol. Biol. 203*, 939–947.
Yeung, A. T., Mattes, W. B., Oh, E., Y., & Grossman, L. (1983) *Proc. Natl. Acad. Sci. U.S.A. 80*, 6157–6161.